Inorganic Chemistry

Article

pubs.acs.org/IC

Thiocyanate Linkage Isomerism in a Ruthenium Polypyridyl Complex

Timothy P. Brewster, Wendu Ding, Nathan D. Schley, Nilay Hazari, Victor S. Batista,* and Robert H. Crabtree*

Department of Chemistry, Yale University, P.O. Box 208107, New Haven, Connecticut 06520-8107, United States

Supporting Information

ABSTRACT: Ruthenium polypyridyl complexes have seen extensive use in solar energy applications. One of the most efficient dye-sensitized solar cells produced to date employs the dye-sensitizer N719, a ruthenium polypyridyl thiocyanate complex. Thiocyanate complexes are typically present as an inseparable mixture of N-bound and S-bound linkage isomers. Here we report the synthesis of a new complex, [Ru(terpy)(tbbpy)SCN][SbF_6] (terpy = 2,2′;6′,2″-terpyridine, tbbpy = 4,4′-di-*tert*-butyl-2,2′-bipyridine), as a mixture of N-bound and S-bound thiocyanate linkage isomers that can be separated based on their relative solubility in ethanol. Both isomers have been characterized spectroscopically and by X-ray crystallography. At elevated temperatures the isomers equilibrate, the product being significantly enriched in the more thermodynamically stable N-bound form. Density functional theory analysis supports our experimental observation that the N-bound isomer is thermodynamically preferred, and provides insight into the isomerization mechanism.

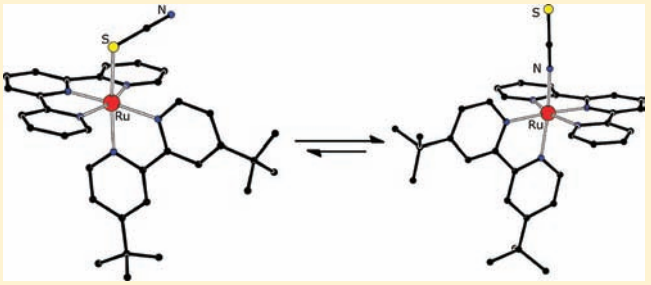

INTRODUCTION

Rising energy costs and mounting concern about the ecological impact of fossil fuel consumption have led to increased interest in solar power. While there are many different strategies for converting solar energy to electricity,[1,2] the majority suffer from high production costs that make them difficult to implement on a large scale. The search for a cheaper alternative led O'Regan and Grätzel to develop the dye-sensitized solar cell (DSSC).[3] Rather than using silicon based materials that give efficient photoresponse but are expensive to purify as semiconductors, DSSCs can instead employ inexpensive nanocrystalline TiO_2 for this purpose. However, the band gap of TiO_2 is not poised to absorb in the visible range of the electromagnetic spectrum, so dye molecules must be adsorbed to the surface of the nanoparticles to act as sensitizers.[4]

Variation of the dye structure causes a vast change in the overall performance of DSSCs.[5] Two of the most efficient dyes, N719 and N749, both ruthenium polypyridyl thiocyanate complexes, (Figure 1)[6,7] give overall conversion efficiencies (η) of 11.2% and 10.4% respectively. Furthermore, it has been shown that substituting thiocyanate with other anionic ligands reduces the overall efficiency of the dye, presumably because of a decrease in visible light absorption.[8]

Thiocyanate is an ambidentate ligand which can bind to a metal through either the nitrogen or the sulfur atoms. For solar cell applications, it has been postulated that the N-bound thiocyanate isomer is preferable. Although charge transfer from electrolyte to dye could be happening in several other ways,[9,10] it has been suggested that the N-bound isomer promotes charge transfer from the iodide redox mediator, which can interact with the soft, sulfur end of the ligand. This is proposed to increase DSSC efficiency.[11,12] As a result of this proposed difference in solar cell efficiency it is useful to know and control the binding mode of thiocyanate in ruthenium polypyridyl systems. In the case of N719 and N749 it has been found that binding through nitrogen is preferred thermodynamically.[8,13] However, in the presence of iodide at elevated temperature, an equilibrium is established between species with coordinated iodide and both N- and S-bound thiocyanate linkage isomers.[14,15]

Linkage isomerization of thiocyanate in ruthenium complexes has been observed previously. In 2008, Freedman and co-workers reported the synthesis of both linkage isomers of [(*para*-cymene)Ru(bpy)SCN]$^+$ (bpy = 2,2′-bipyridine).[16] They were able to confirm the formation of each isomer by NMR spectroscopy, calculate equilibrium parameters for the system, and isolate each isomer by column chromatography. This is the only previous report in which both linkage isomers of a ruthenium thiocyanate complex have been characterized crystallographically. In fact it is quite rare to find crystallographic data for any S-bound ruthenium thiocyanate complexes.[17−19]

In a system more closely related to DSSC applications, Grätzel and co-workers documented linkage isomerization in the anionic complexes [Ru(bmipy)(dcbpy)SCN]$^-$ and [Ru(ph-bmipy)(dcbpy)SCN]$^-$ (bmipy = 2,6-bis(1-methylbenzimidazol-2-yl)-pyridine, ph-bmipy = 2,6-bis(1-methylbenzimidazol-2-yl)-4-phenylpyridine, dcbpy = 4,4′-dicarboxy-2,2′-bipyridine).[14] The linkage isomers were distinguished by NMR and IR spectroscopy, and the different solubility of the two isomers was noted. However, neither isomer was obtained in pure form. After 24 h

Received: May 6, 2011
Published: November 8, 2011

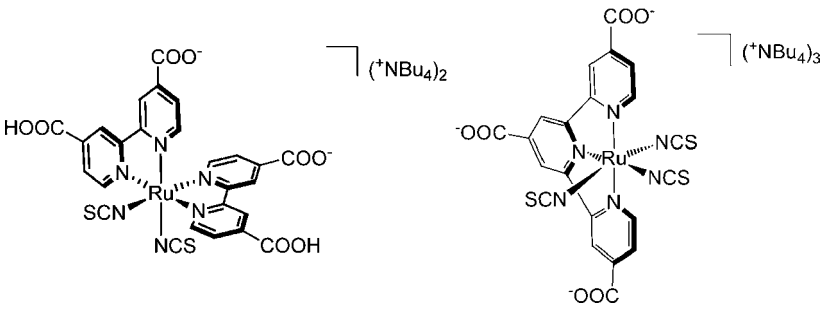

Figure 1. N719 and N749.

Scheme 1. Synthesis of the Title Complex [Ru(terpy)(tbbpy)(SCN)][SbF$_6$][22]

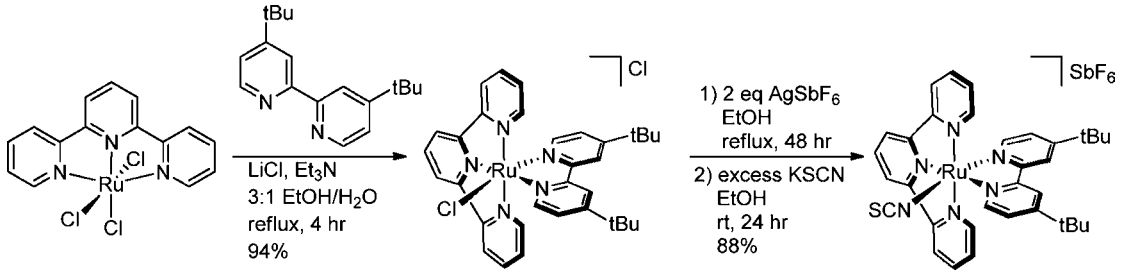

refluxing in methanol, 5% of the thermodynamically disfavored S-bound isomer remained. Grätzel and co-workers have also demonstrated that N719 exists as a mixture of isomers.[14] They subsequently demonstrated that isomerization of N719 occurs upon illumination in solar cells containing the dye under standard operating conditions in the presence of an iodide electrolyte.[15]

Here we report the synthesis of a new compound, [Ru(terpy)(tbbpy)SCN][SbF$_6$] (terpy = 2,2′;6′,2″-terpyridine, tbbpy = 4,4′-di-*tert*-butyl-2,2′-bipyridine) that can be isolated as either the N-bound or the S-bound isomer. Both isomers have been characterized spectroscopically and by X-ray crystallography; the first time both linkage isomers of a purely polypyridyl ruthenium thiocyanate complex have been structurally characterized. At elevated temperatures, equilibration of the two isomers allows the thermodynamic parameters for the system to be determined experimentally, and these have been compared with computational results. In addition, a density functional theory (DFT) based investigation into the mechanism of isomerization has been performed.

RESULTS AND DISCUSSION

[Ru(terpy)(tbbpy)Cl]Cl[20,21] was prepared from Ru(terpy)Cl$_3$[22] by a modification of the literature procedure for the preparation of [Ru(terpy)(bpy)Cl]Cl.[23] In our synthesis, Ru(terpy)Cl$_3$, LiCl, and triethylamine were treated with 4,4′-di-*tert*-butyl-2,2′-bipyridine in 75% aqueous ethanol to afford [Ru(terpy)(tbbpy)Cl]Cl in 94% isolated yield. Treatment of [Ru(terpy)(tbbpy)Cl]Cl with excess silver hexafluoroantimonate led to precipitation of silver chloride in refluxing ethanol and gave what is presumed to be a solvento species [Ru(terpy)(tbbpy)(solv)][SbF$_6$]$_2$. After filtration, potassium thiocyanate was added to the filtrate. The reaction mixture was concentrated in vacuo and the suspension cooled, leading to the precipitation of [Ru(terpy)(tbbpy)SCN][SbF$_6$] as a mixture of N- and S-bound isomers (Scheme 1). After washing the precipitate with water, subsequent concentration of the filtrate in vacuo led to precipitation of a second crop of product.

The ^{1}H NMR spectra of both crops of product indicated that a mixture of two different complexes was present. On the basis of evidence discussed below, we believe that the two complexes are the N- and S-bound thiocyanate isomers, each with distinct NMR resonances. The isomeric ratio in each crop of the precipitate was found to depend on the amount of solvent left in the reaction vessel, with the N-bound isomer present in greater proportion in the first crop than the more-soluble S-bound isomer. A mixture of the two isomers can be obtained in 88% combined yield. For simplicity, SCN in any formula denotes a material with unknown binding mode or containing a mixture of isomers; *S*-SCN and *N*-SCN denote the individual isomers.

Our assignment of the two isomers in the ^{1}H NMR spectrum of the product mixture is consistent with that in a previous complex of similar structure, [Ru(bmipy)(dcbpy)SCN]$^+$.[14] By analogy with prior work, the proton signals at δ9.42 and δ9.72 correspond to the 6H proton of the dipyridyl ligand proximal to the thiocyanate in [Ru(terpy)(tbbpy)SCN][SbF$_6$] (Figure 2).

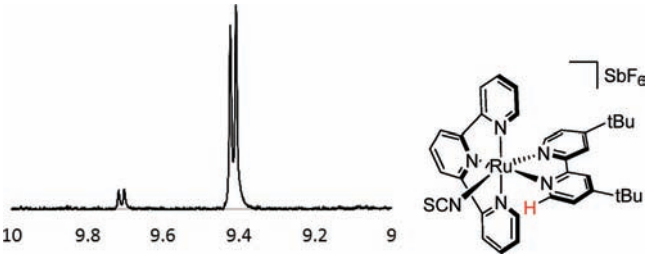

Figure 2. Representative ^{1}H NMR spectrum from δ9.0 to δ10.0 in d_6-DMSO of linkage isomers of [Ru(terpy)(tbbpy)SCN][SbF$_6$]. The peak at δ9.42 corresponds to the 6H proton, illustrated at right, in the N-bound isomer. The peak at δ9.72 corresponds to the 6H proton in the S-bound isomer. For the full spectrum see Supporting Information.

The proton peak for the N-bound isomer is expected to be shifted upfield from the S-bound isomer.[14] The assignment has also been confirmed by spectra of the pure isomers (vide infra; see Supporting Information).

dx.doi.org/10.1021/ic200950e | *Inorg. Chem.* 2011, 50, 11938–11946

There are two possible explanations for the isomeric ratio obtained from our synthetic route: (i) the reaction is under thermodynamic control and the product ratio observed is determined by the relative energies of the isomers, or (ii) the reaction is under kinetic control and the product ratio is determined by selectivity in the binding of thiocyanate to Ru. A series of experiments were performed to distinguish between the two possibilities.

Upon heating a sample of [Ru(terpy)(tbbpy)SCN][SbF_6] in dimethyl sulfoxide (DMSO) to temperatures above 110 °C a shift in the isomeric ratio is observed by ^{1}H NMR spectroscopy (see Experimental Details). When samples are left to stand at room temperature however, the isomeric ratio is invariant, indicating that elevated temperatures are required to overcome the activation barrier for isomerization. A series of isomerization reactions were performed at different temperatures to determine the relative free energies of the isomers. These reactions were carried out in the presence of excess thiocyanate, which was added to prevent the formation of a solvent-bound ruthenium species with dissociated thiocyanate. Control experiments indicated that addition of excess thiocyanate does not affect the equilibrium ratio of the two linkage isomers. A Van't Hoff plot (Figure 3) indicates that the

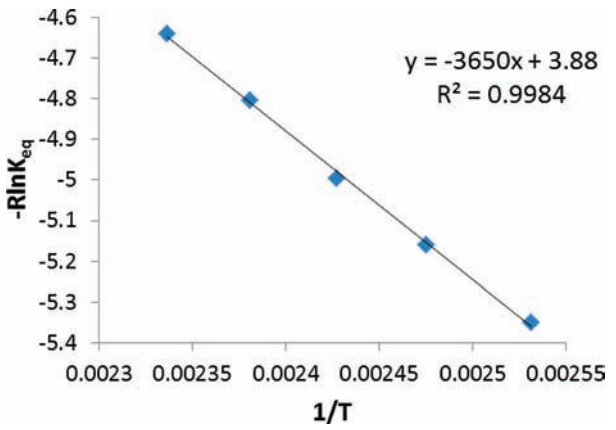

Figure 3. Van't Hoff plot of average equilibrium data obtained for the reaction [Ru(terpy)(tbbpy)*S*-SCN][SbF_6] = [Ru(terpy)(tbbpy)*N*-SCN][SbF_6].

N-bound isomer is favored enthalpically by 3.65 ± 0.75 kcal/mol while the entropy change on isomerization is −3.88 ± 1.81 cal/K·mol (see Supporting Information for regression analysis). This small change in entropy is not surprising given the small structural change on isomerization.

On the basis of our thermodynamic data, the N:S-bound isomeric ratio of roughly 3:2 (vide infra) observed in the initial synthetic reaction product is inconsistent with a thermodynamically controlled process, implying that the reaction must be kinetically controlled. To test this, a reaction was conducted in d_4-methanol. After chloride abstraction from [Ru(terpy)(tbbpy)Cl]Cl at room temperature with silver hexafluoroantimonate, potassium thiocyanate was added to the sample in an NMR tube without filtering and the reaction was monitored by ^{1}H NMR spectroscopy (Figure 4). The thiocyanate complex forms rapidly under these conditions, as after only 15 min a precipitate is visible and signals corresponding to both isomers can be seen. The S-bound form is present in solution at roughly 6-fold excess, though subsequent analysis of the precipitate shows that it is heavily enriched with N-bound isomer. Dissolution of the whole product sample in DMSO gives an isomeric ratio close to 1:1, consistent with binding of thiocyanate with little kinetic preference.

Results obtained on a preparative scale also support kinetic control of the reaction. Beginning with 250 mg of [Ru(terpy)(tbbpy)Cl]Cl, 293 mg of product is obtained; of which approximately 208 mg is the N-bound isomer, as calculated from the ^{1}H NMR data. This corresponds to 62% yield of N-bound isomer, consistent with our findings from the NMR experiment.

On the basis of the experimentally determined activation barrier for isomerization and the ratio of products seen by NMR, we conclude that the N/S ratio obtained is the kinetic product ratio. From the NMR tube experiment described above it was clear that the two isomers have different solubility. We thought that by varying the amount of solvent we could control the ratio of S-bound to N-bound isomers precipitated. Indeed, if a small amount of solvent is removed in vacuo to obtain the first crop of product (see Experimental Details) the pure N-bound isomer is isolated, albeit in low yield. Alternatively, if a large amount of solvent was removed to obtain the first crop of product, all of the N-bound isomer precipitates. As a result, the product obtained from the second crop was found to be purely S-bound isomer, also in low yield. Isolated yields of pure product isomers are 34% (based on starting material) for the N-bound and 4.5% for the S-bound isomer. This is a new method of purifying the linkage isomers, although we do not know if it will be general.

With pure species in hand further spectroscopic comparison was now possible. A diagnostic IR stretching band at around 2100 cm^{-1} can be unambiguously assigned to the C−N stretching mode of the coordinated thiocyanate ligand since there are no other IR active modes in this region of the spectrum (Figure 5; full spectrum in Supporting Information). This band occurs at a slightly higher frequency (2108 cm^{-1}, nujol mull) for the S-bound isomer compared with the N-bound isomer (2102 cm^{-1}, nujol mull and diffuse reflectance). A small difference in frequency is not unexpected, and has been observed in other thiocyanate complexes.[16,24] However, when both isomers are present in comparable amount, the peaks are not resolved. In particular, the peak corresponding to the S-bound isomer is easily obscured by the relatively stronger absorption of the N-bound isomer. In some cases a shoulder at 2050 cm^{-1} is observed and can be misleading. This has now been unambiguously assigned to free thiocyanate by addition of potassium thiocyanate to a sample containing a mixture of isomers (See Supporting Information).

Alternatively, the C−S stretching mode could be useful to determine the bonding of thiocyanate. This stretching frequency, predicted by DFT (vide infra) to be at 868 cm^{-1} for the N-bound isomer and at 705 cm^{-1} for the S-bound isomer, is expected to show a greater difference between the two isomers if the change in binding mode alters the bonding within the ligand. However, this section of the IR spectrum cannot be rigorously assigned because of the large number of peaks present. Thus the C−N stretching mode, in this case, proves to be more instructive.

Computational data support this observed difference in IR stretching frequency (Figure 5) for the two isomers. The C−N stretch for the S-bound isomer is calculated to occur at a higher frequency than that of the N-bound isomer. Furthermore, the calculated intensity of the C−N stretch in the N-bound isomer is 13 times stronger than in the S-bound isomer, which is

dx.doi.org/10.1021/ic200950e | *Inorg. Chem.* 2011, 50, 11938–11946

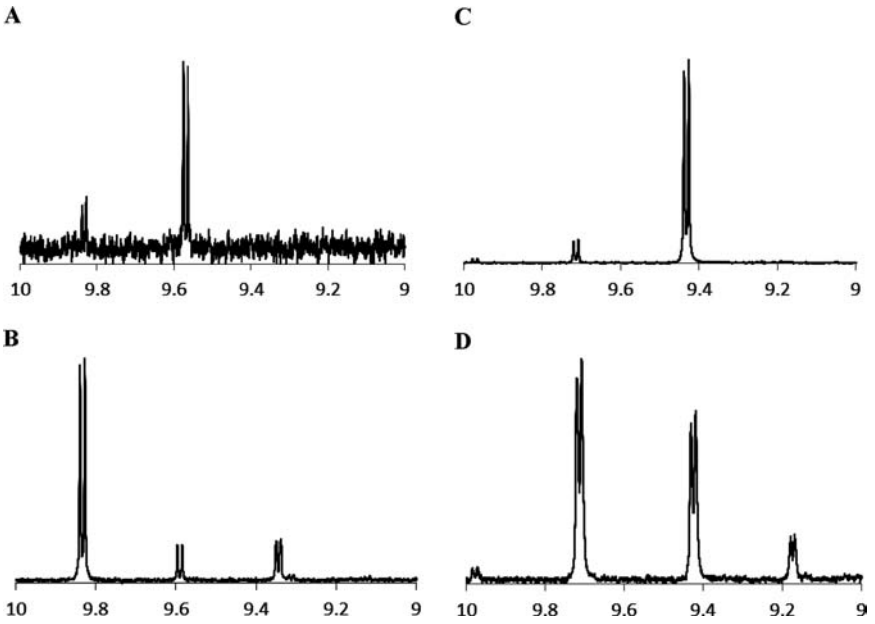

Figure 4. Selected ^{1}H NMR spectra. (A) Crude product obtained from the first crop of a representative synthesis (See Experimental Details). Recorded in d_4-methanol. The predominant species is the N-bound isomer. (B) NMR tube reaction mixture after 19 h in d_4-methanol. The predominant species is the S-bound isomer. The signal at δ9.35 is the solvento complex. (C) Precipitate from NMR tube reaction. (d_6-DMSO) The predominant species is the N-bound isomer. The signal at δ9.98 is unreacted starting material. (D) NMR tube reaction mixture entirely redissolved in d_6-DMSO. Integration shows similar amounts of N-bound and S-bound isomers. The signal at δ9.18 is the methanol complex.

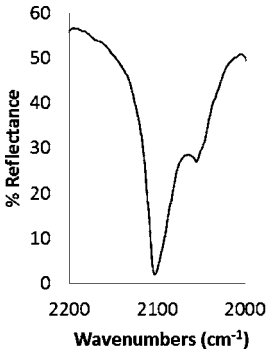

Isomer	Measured (cm^{-1})	Calculated (cm^{-1})
N-bound	2102	2142
S-bound	2108	2200

Figure 5. Diffuse Reflectance (KBr) IR spectrum of [Ru(terpy)-(tbbpy)SCN][SbF_6] in the C−N stretching region of a mixture of isomeric products. By ^{1}H NMR spectroscopy, the sample ratio is 3:1 N-bound:S-bound. The peak energy in wavenumbers of both measured and calculated spectra are shown at right. The shoulder at 2050 cm^{-1} corresponds to free thiocyanate (see Supporting Information). For computational methods see Experimental Details.

consistent with only one peak being observed when an approximately equimolar mixture of isomers is present. Calculations also show that the C−N bond length in the N-bound isomer is 1.181 Å while in the S-bound isomer it is 1.166 Å, which is consistent with IR data.

The two isomers give distinct UV/vis spectra. When dissolved in DMSO, both isomers display strong absorption below 650 nm. Each isomer features a broad peak centered just below 500 nm and a shoulder around 440 nm. Interestingly, the λ_{max} is bathochromically shifted by 7 nm (297 cm^{-1}) from 482 nm (ε = 6400 M^{-1} cm^{-1}) for the S-bound isomer to 489 nm (ε = 5800 M^{-1} cm^{-1}) for the N-bound isomer (Figure 6). A slight decrease in molar absorptivity is observed on moving from S-bound to N-bound. However, in both cases the large molar absorptivity values measured are consistent with this broad peak corresponding to a charge transfer band. It is possible that the observed red shift upon moving from S-bound to N-bound in absorption is beneficial for solar cell applications as it allows for a more complete coverage of the visible spectrum.

A time-dependent DFT (TD-DFT) simulation has also been run to computationally predict the UV/vis spectrum of each isomer (See Experimental Details). Predicted UV/vis spectra are shown in Figure 6. Calculated spectra support the experimental observation of a bathochromic shift in moving from the S-bound isomer to the N-bound isomer with only a slight decrease in molar absorptivity. For [Ru(terpy)(bpy)*S*-SCN]$^+$, which is used as a computational analogue to the title complex (vide infra), the calculated λ_{max} = 433 nm (ε = 5578); while for [Ru(terpy)(bpy)*N*-SCN]$^+$ the calculated λ_{max} = 449 nm (ε = 5397).

The broad peak centered at λ_{max} is predicted to incorporate excitations from occupied orbitals in the range of HOMO-5 to HOMO and unoccupied orbitals in the range of LUMO to LUMO+5 for both isomers. As expected from the high molar extinction coefficient, the calculated transition is predominantly a charge transfer band. In both cases the charge transfer is mostly from a metal-centered d-orbital to an orbital based on one of the polypyridyl ligands. Occupied metal-centered orbitals involved in the charge transfer excitation do show some thiocyanate character. (Figures 7A and 7B) Interestingly, in the case of [Ru(terpy)(bpy)*N*-SCN]$^+$, there appears to be more involvement of the thiocyanate ligand in metal centered orbitals than is observed for [Ru(terpy)(bpy)*S*-SCN]$^+$. This can be seen in Figure 7C which shows a transition from a metal-centered orbital with very little thiocyanate involvement. An analogous excitation was not found for the N-bound isomer. This may account for the slight difference in λ_{max} between the two isomeric complexes.

Further characterization of both isomers was obtained through X-ray crystallography (Figure 8). This is only the second time in which crystal structures of both linkage isomers

dx.doi.org/10.1021/ic200950e | *Inorg. Chem.* 2011, 50, 11938–11946

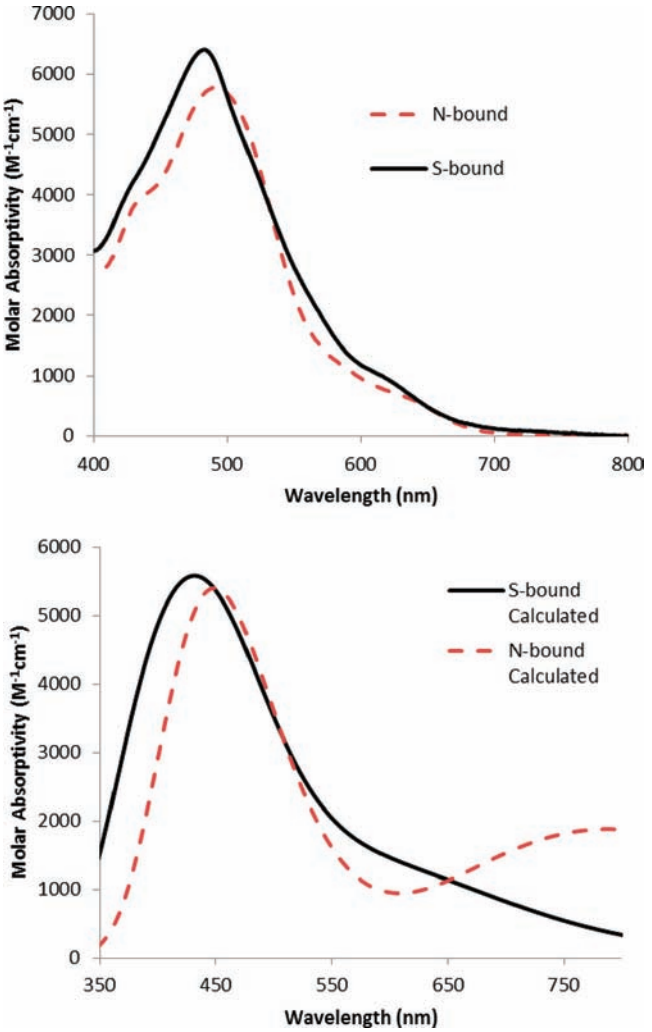

Figure 6. UV/vis spectra of isomers. Top: Measured in DMSO solution. Black solid line: S-bound isomer, λ_{max} = 482 nm (ε = 6400 M^{-1} cm^{-1}), shoulder at 434 nm. Red dashed line: N-bound isomer, λ_{max} = 489 nm (ε = 5800 M^{-1} cm^{-1}), shoulder at 440 nm. Bottom: Calculated UV/vis spectra from TD-DFT. Black solid line: S-bound isomer; λ_{max} = 433 nm (ε = 5578). Red dashed line: N-bound isomer; λ_{max} = 449 nm (ε = 5397).

have been determined for a single ruthenium complex.[16] Crystals were obtained by diffusion of pentane into a saturated 1,2-dichloroethane solution of each pure isomer. For the bent S-bound isomer a Ru−S bond length of 2.470(3) Å, a S(1)−C(34) bond length of 1.613(19) Å, and a C(34)−N(6) bond length of 1.19(2) Å were measured. The Ru−S−C(34) bond angle was 106.7(5)°. For the linear N-bound isomer a Ru−N bond length of 2.067(4) Å, a S(1)−C(34) bond length of 1.640(5) Å, and a C(34)−N(6) bond length of 1.133(7) Å were obtained. The Ru−N(6)−C(34) bond angle was 175.7(6)°. Bond lengths and angles for each isomer are consistent with those obtained previously for ruthenium thiocyanate linkage isomers.[16−19,25,26]

The apparent C−N bond length determined from X-ray crystallography is shorter in the N-bound isomer than in the S-bound isomer, a finding which is contrary to the calculated C−N distances and to the measured IR spectra reported above. This is probably due to the low-quality of the crystal used for the structure determination of the S-bound isomer, which defied our efforts to grow better ones. Additionally, in a previous report where both isomers were crystallized,[16] identical C−N bond lengths were found for both isomers even though a 10 wavenumber difference was observed by IR spectroscopy for the C−N stretching frequency. In both cases the difference in bond lengths and IR stretching frequencies between the two isomers is very small.

The experimentally observed thiocyanate isomerization was also modeled computationally. Two separate systems were considered: the full experimental system [Ru(terpy)(tbbpy)-SCN]$^+$, and a computationally simpler system [Ru(terpy)-(bpy)SCN]$^+$. Removal of the *tert*-butyl groups did not have an appreciable effect on calculated energies and geometries (Supporting Information, Table S11). Different basis sets provided similar relaxed geometries, all in good agreement with X-ray crystallography. The gas phase Ru−N−C bond angle in [Ru(terpy)(bpy)*N*-SCN]$^+$ was 168°, and that in [Ru(terpy)-(tbbpy)*N*-SCN]$^+$ was 175°. The Ru−S−C bond angles in both [Ru(terpy)(bpy)*S*-SCN]$^+$ and [Ru(terpy)(tbbpy)*S*-SCN]$^+$ were 104°. These calculated values are consistent with experimental values obtained from crystallography (vide supra).

Solvation enthalpies and free energies were calculated for [Ru(terpy)(bpy)SCN]$^+$ in DMSO based on the SMD model. Using the LANL2DZ basis set for Ru, 6-31++G(d,p) for C and H atoms and cc-pVTZ for N and S atoms thermodynamic parameters for the isomerization reaction [Ru(terpy)(tbbpy)*S*-SCN][SbF_6] ↔ [Ru(terpy)(tbbpy)*N*-SCN][SbF_6] were calculated. It was found that ΔH°_{sol} = 7.18 kcal/mol and ΔG°_{sol} = 8.18 kcal/mol. A comparison to results based on other combinations of basis set and solvation models is given in the Supporting Information, Table S11.

Interestingly, all values computed from solvation models give larger calculated enthalpy changes than the gas phase value calculated with the same basis set. Also, in all cases, the change in entropy upon isomerization is calculated to have an opposite sign from that determined experimentally. This could be because solvent is being modeled by a continuum model rather than explicit solvent molecules. It is possible that there is an interaction between the bound thiocyanate ligand and its closest neighboring molecules of DMSO which would vary depending on whether the hard, nitrogen end or the soft, sulfur end of the ligand is exposed. Reorganization of the solvent because of this interaction could account for the small discrepancy between the calculated and the measured thermodynamic parameters. Unfortunately, a calculation with explicit solvent is very difficult in this case. This is because the isomerization reaction being modeled was not run with exclusion of water. Thus the exact nature of the solvent around the complexes is not well-defined, and it would be impossible to guarantee that any model is an accurate reflection of the actual system. However, even with this simplification, computed values for ΔH°_{sol} and ΔG°_{sol} are in reasonable agreement with experiment.

With thermodynamic parameters in hand, a computational investigation of the mechanism of isomerization was undertaken. An energy profile of the minimized structure of [Ru(terpy)(bpy)SCN]$^+$ calculated with various fixed Ru−N bond distances is shown in Figure 9. A similar figure for [Ru(terpy)(tbbpy)SCN]$^+$ can be found as the Supporting Information, Figure S12. The minimized structure at point 2 (Figure 9) has a Ru−N distance of 2.99 Å, a Ru−C distance of 3.36 Å, and a Ru−S distance of 4.37 Å. These distances are all too long to be considered bonding interactions and indicates a dissociative mechanism. Supporting this, a transition state

dx.doi.org/10.1021/ic200950e | *Inorg. Chem.* 2011, 50, 11938−11946

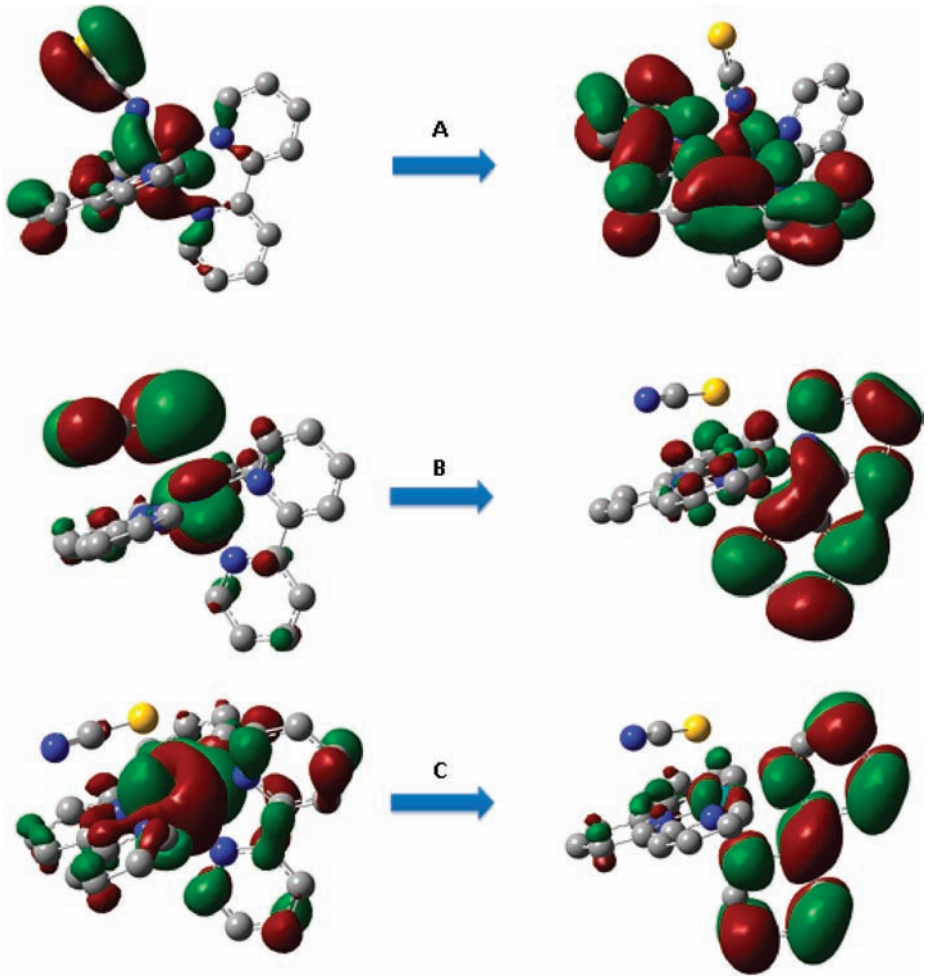

Figure 7. TD-DFT generated orbitals of representative λmax transitions. A: HOMO-4 to LUMO+1 for N-bound isomer; B: HOMO to LUMO+3 for S-bound isomer; C: HOMO-2 to LUMO for S-bound isomer.

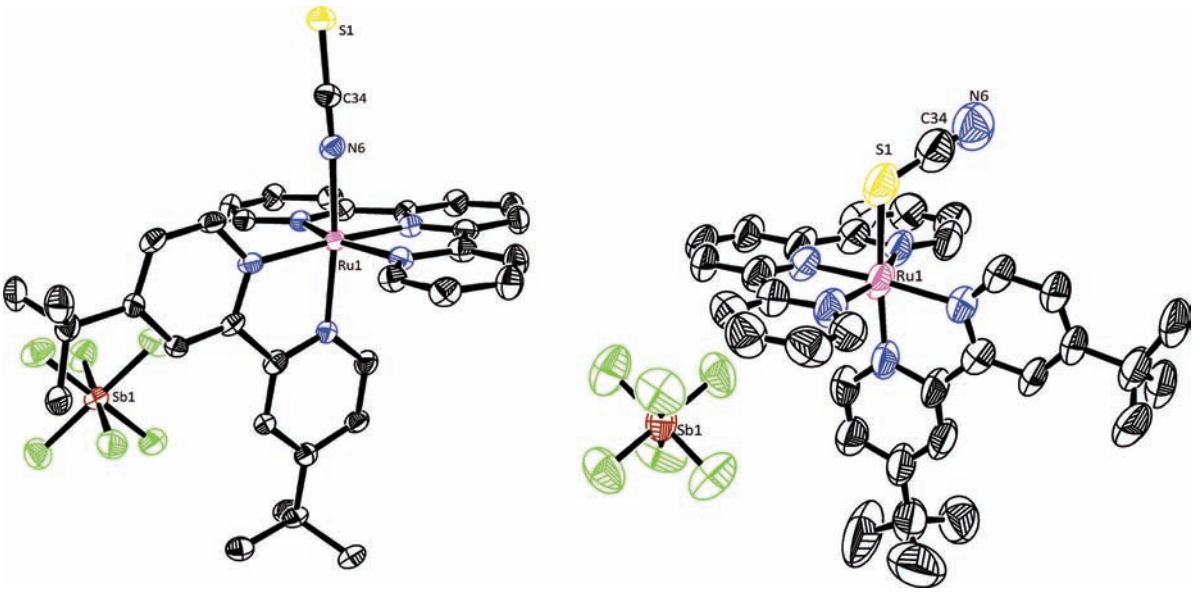

Figure 8. ORTEP of [Ru(terpy)(tbbpy)SCN][SbF_6]. Left: N-bound Isomer. Right: S-Bound Isomer. Thermal ellipsoids shown at 50% probability. Hydrogen atoms are omitted for clarity.

search (QST2) centered at point 1 was done to look for a possible π-bound intermediate. However, this yielded a minimized structure higher in energy (point C) than the sum of the two free solvated ions $[Ru(terpy)(bpy)]^{2+}$ and SCN^- (point D) consistent with a fully dissociative mechanism. It is also likely that a dissociative mechanism is favored by the highly

dx.doi.org/10.1021/ic200950e | *Inorg. Chem.* 2011, 50, 11938–11946

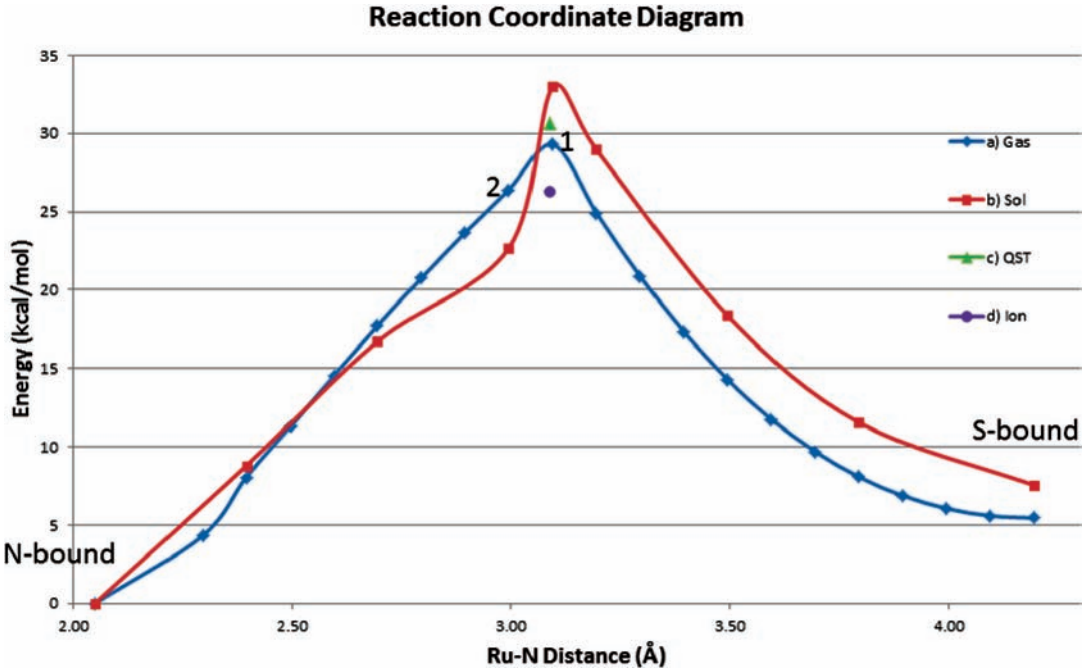

Figure 9. Transition state scan for $[Ru(terpy)(bpy)SCN]^+$ from S-bound to N-bound. (a) Gas: transition state scans in gas phase; (b) Sol: solvation energy correction on selected geometries from scans; (c) QST: result from transition state search (with solvation energy correction); (d) Ion: energy (with solvation energy correction) of free double cation of $[Ru(terpy)(bpy)]^{2+}$ and free SCN^- anion. For computational methods see Experimental Details.

polar DMSO solvent. This can be seen at point 2 where the metal and ligand are far enough apart to be considered not bonded. Adding solvation to the calculation significantly lowers the calculated energy at this point. Finally, the calculated energy of the fully dissociated ions (Point D) is roughly 25 kcal/mol higher than that of the calculated thermodynamic product $[Ru(terpy)(bpy)N\text{-}SCN]^+$. This is consistent with the elevated temperatures required experimentally to drive the isomerization reaction and the lack of equilibration under ambient conditions.

■ CONCLUSIONS

We have synthesized a new compound, $[Ru(terpy)(tbbpy)SCN][SbF_6]$, as a mixture of thiocyanate linkage isomers. By selectively precipitating the N- and S-bound isomers from ethanol, each isomer has been isolated in pure form and characterized spectroscopically. Additionally, crystallographic data confirming the structural assignment has been obtained. Isomerization between the two isomers can be achieved at elevated temperatures, leading to a product which is enriched in the thermodynamically favored N-bound isomer. DFT simulations confirm the thermodynamic parameters obtained experimentally and suggest a dissociative mechanism for the isomerization. The ability to obtain a purely N-bound ruthenium thiocyanate complex, as outlined here, may prove useful in future studies on dye sensitized solar cells.

■ EXPERIMENTAL DETAILS

$Ru(terpy)Cl_3$ was synthesized by a literature method.[22] Ethanol, $RuCl_3 \cdot 3H_2O$, terpyridine, 4,4′-di-*tert*-butyl-2,2′-bipyridine, and potassium thiocyanate were purchased from commercial sources and used without further purification. Silver hexafluoroantimonate was purchased from Alfa Aesar and stored in the dark in a vacuum desiccator prior to use. Deuterated solvents were purchased from Cambridge Isotope Laboratories and used as received. ^1H NMR spectra were recorded on a 400 MHz Bruker spectrometer and referenced to the residual solvent peak (δ in ppm, J in Hz). ^{13}C NMR spectra were recorded on a 500 MHz Varian spectrometer and referenced to the solvent peak. IR spectra were recorded on a Nicolet 6700 FT-IR spectrometer in diffuse reflectance mode or as a nujol mull in KBr plates. UV/vis spectra were recorded as a dilute solution in DMSO on a Varian Cary 3 spectrophotometer. Elemental analysis was performed by Robertson Microlit Laboratories (Ledgewood, NJ).

$[Ru(terpy)(tbbpy)(Cl)]Cl \cdot H_2O$. This compound was prepared by a modification of the literature procedure for the synthesis of $[Ru(terpy)(bpy)Cl]Cl$.[23] Synthesis of $[Ru(terpy)(tbbpy)Cl]Cl$ has been previously reported in a similar fashion.[20,21] 1.00 g $Ru(terpy)Cl_3$ (2.27 mmol), 100 mg lithium chloride (2.43 mmol), and 610 mg 4,4′-di-*tert*-butyl-2,2′-bipyridine (2.27 mmol) were dissolved in 200 mL of 3:1 ethanol:water. One milliliter of triethylamine (7.17 mmol) was then added. The mixture was sparged with nitrogen and then refluxed for 4 h. The resulting suspension was filtered hot in air and the filtrate collected. The solution volume was then reduced to 25 mL on a rotary evaporator, and the resulting suspension chilled in a refrigerator overnight. The black precipitate was collected by filtration and washed with excess water and diethyl ether. Isolated yield 1.43 g (2.13 mmol, 94%). ^1H NMR (400 MHz, DMSO) δ 9.98 (d, J = 6.1 Hz, 1H), 8.93 (d, J = 1.7 Hz, 1H), 8.80 (d, J = 8.1 Hz, 2H), 8.68 (d, J = 8.0 Hz, 2H), 8.66 (d, J = 1.9 Hz, 1H), 8.20 (t, J = 8.1 Hz, 1H), 8.09 (dd, J = 6.0, 1.9 Hz, 1H), 7.98 (td, J = 7.9, 1.4 Hz, 2H), 7.61 (d, J = 4.8 Hz, 2H), 7.39 (m, 2H), 7.13 (d, J = 6.2 Hz, 1H), 7.06 (dd, J = 6.2, 2.0 Hz, 1H), 1.59 (s, 9H), 1.22 (s, 9H). ^{13}C NMR (126 MHz, DMSO) δ 160.59, 159.59, 158.43, 157.97, 157.64, 155.29, 151.76, 151.43, 150.95, 136.89, 133.40, 127.48, 123.89, 123.67, 123.39, 122.57, 121.02, 120.93, 35.56, 35.08, 30.44, 29.90. Elemental Analysis for $C_{33}H_{37}Cl_2N_5ORu$: Calcd: C: 57.30, H: 5.39, N: 10.13. Found: C: 56.95, H: 5.17, N: 9.96.

$[Ru(terpy)(tbbpy)SCN][SbF_6]$. A 250 mg portion of $[Ru(terpy)(tbbpy)Cl]Cl$ (0.371 mmol) and 500 mg of silver hexafluoroantimonate (1.46 mmol, 3.94 equiv.) were stirred for 48 h in the dark under nitrogen in 25 mL of absolute ethanol at reflux. The resulting suspension was filtered through Celite in air to remove silver chloride. The Celite was washed with small portions of 95% ethanol. To the resulting solution was added 175 mg of potassium thiocyanate (1.71 mmol, 4.67 equiv). The mixture was then stirred at room temperature overnight. The resulting suspension was reduced in volume to

dx.doi.org/10.1021/ic200950e | Inorg. Chem. 2011, 50, 11938–11946

approximately 20 mL on a rotary evaporator, and the suspension placed in a refrigerator overnight. The resulting dark red solid was filtered and washed with cold water and diethyl ether. A second crop of product was obtained by concentration of the filtrate in vacuo to approximately 10 mL and subsequent filtration. The initial crop of product was obtained as a mixture of N-bound and S-bound isomers (in a ratio dependent on final solvent volume) enriched in N-bound isomer. The second crop is obtained as a mixture enriched in S-bound isomer. A large residual solvent volume for the first crop yields high selectivity for the N-bound isomer in smaller yield in the first crop, while a small residual solvent volume for the first crop yields a high proportion of S-bound isomer in small yield as the second crop. In the extreme case, pure N-bound isomer, as measured by ^{1}H NMR spectroscopy, can be isolated in the first crop by removal of solvent until solid just begins to precipitate, Alternatively, removal of solvent almost to dryness to obtain the first crop of product allows for total precipitation of the N-bound isomer. Thus pure S-bound product can be obtained from the second crop of product in this manner. Isolated yield (sum of both fractions): 293 mg (0.327 mmol, 88%) Crystals for X-ray analysis were obtained by slow diffusion of pentane into a saturated solution of pure isomer in 1,2-dichloroethane. ^{1}H NMR for N-bound isomer (400 MHz, DMSO) δ 9.42 (d, J = 5.9 Hz, 1H), 8.95 (d, 1H), 8.88 (d, J = 8.1 Hz, 2H), 8.75 (d, J = 7.8 Hz, 2H), 8.69 (d, 1H), 8.33 (t, J = 8.1 Hz, 1H), 8.19 (dd, J = 6.0, 2.0 Hz, 1H), 8.07 (m, 2H), 7.67 (d, J = 4.7 Hz, 2H), 7.46 (m, 2H), 7.12 (s, 2H), 1.59 (s, 9H), 1.24 (s, 9H). ^{13}C NMR for N-bound isomer (126 MHz, DMSO) δ 159.68, 158.92, 156.46, 155.81, 155.66, 153.52, 150.58, 149.33, 148.91, 136.25, 133.43, 131.71, 126.47, 123.14, 122.62, 121.98, 121.65, 119.89, 119.51, 34.11, 33.62, 28.85, 28.33. ^{1}H NMR for S-bound isomer (400 MHz, DMSO) δ 9.72 (d, J = 6.0 Hz, 1H), 8.93 (s, 1H), 8.85 (d, J = 8.1 Hz, 2H), 8.71 (m, 3H), 8.27 (t, J = 8.1 Hz, 1H), 8.11 (dd, J = 6.0, 2.0 Hz, 1H), 8.01 (t, J = 7.8 Hz, 2H), 7.64 (d, J = 5.4 Hz, 2H), 7.43 (m, 2H), 7.17 (d, 2H), 1.58 (s, 9H), 1.23 (d, J = 4.5 Hz, 9H). ^{13}C NMR for S-bound isomer (126 MHz, DMSO) δ 161.14, 160.84, 157.96, 157.00, 156.76, 155.56, 152.07, 151.63, 150.05, 137.39, 134.37, 127.92, 124.44, 124.09, 123.74, 123.14, 121.56, 121.07, 119.36, 35.56, 35.20, 30.34, 29.86. IR: $\nu_{C=N}$ (N-bound) 2102 cm^{-1}, $\nu_{C=N}$ (S-bound) 2108 cm^{-1}. Elemental Analysis for $C_{34}H_{35}N_6F_6RuSSb$: Calculated: C 45.55, H: 3.93, N: 9.37. Found: C: 45.71, H: 3.83, N: 9.32.

Procedure for Van't Hoff Experiment. Four milligrams of [Ru(terpy)(tbbpy)SCN][SbF_6] was dissolved in an NMR tube in d_6-DMSO. Excess potassium thiocyanate (10 mg) was then added. The sample was heated to the desired temperature in an oil bath for 2.5 h and then analyzed by ^{1}H NMR after rapid cooling to room temperature. Isomeric ratios were determined by integrating the proton signals at δ9.72 ppm for the S-bound isomer and δ9.42 ppm for the N-bound isomer. Each measurement was repeated in duplicate, and the average value of the isomeric ratio was used to determine thermodynamic parameters. No further isomerization was observed if the solutions were heated for longer than 2.5 h at the set temperature.

Procedure for NMR Tube Reaction. Four milligrams of [Ru(terpy)(tbbpy)Cl]Cl was dissolved in a Schlenk flask in d_4-methanol under nitrogen. To the flask was then added excess silver hexafluoroantimonate (15 mg) in the dark. After 12 h, the solution was equally divided into two different NMR tubes and excess solid potassium thiocyanate (8 mg) added to each. The tubes were then shaken to ensure mixing. ^{1}H NMR spectra (500 MHz, Bruker) were then recorded 15 min after mixing and 19 h after mixing. One sample was then decanted and the precipitated solid redissolved in d_6-DMSO. A second sample was evaporated to dryness under vacuum and then redissolved in d_6-DMSO. ^{1}H NMR spectra then were obtained of the two resulting samples.

Molar Absorptivity Measurement. Molar absorptivities at the absorption maxima were determined at two separate concentrations for each isomer, and the average value was taken. For the S-bound isomer 0.11 mM and 0.056 mM solutions were used while for the N-bound isomer spectra were recorded at concentrations of 0.089 mM and 0.045 mM in a 1.0 cm quartz cuvette.

Computational Methods. DFT calculations were carried out using the Gaussian 09 package[27] with the B3LYP functional. Various combinations of basis sets were applied to the complex systems. LANL2DZ was used as basis set for valence and core electrons in Ru in all instances. 6-31++G(d,p) and cc-pVTZ were used for nonmetal atoms in varying combinations as shown in Supporting Information, Figure S11.

Optimized structures were obtained in gas phase, after which the solvation energies were computed. The Born−Haber cycle (Figure 10)

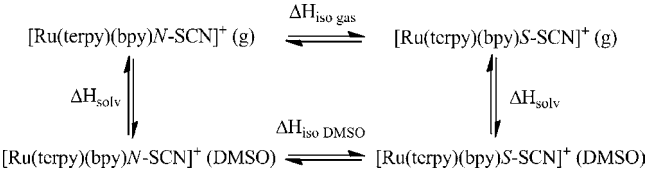

Figure 10. Born−Haber Thermodynamic Cycle used for calculations of enthalpy change.

was then utilized to obtain the change in enthalpy (ΔH) and free energy (ΔG) of the isomerization in solution phase as follows:

$$\Delta H_{sol} = \Delta H_g - \Delta H_{sol}(N) + \Delta H_{sol}(S)$$

and

$$\Delta G_{sol} = \Delta G_g - \Delta G_{sol}(N) + \Delta G_{sol}(S)$$

Solvation energies were computed using both IEFPCM[28] and SMD[29] continuum solvation models with DMSO as solvent.

UV/vis simulations were run using optimized geometries calculated as described above. Single-point TD-DFT calculations were then run using the B3LYP functional and LANL2DZ basis set for ruthenium, 6-31++G(d,p) for carbon and hydrogen, and cc-pVTZ for nitrogen and sulfur for both isomers.

■ ASSOCIATED CONTENT

Ⓢ Supporting Information

NMR spectra for all synthesized compounds, IR spectra for [Ru(terpy)(tbbpy)SCN][SbF_6], crystallographic methods and data, raw data for Van't Hoff experiment, thermodynamic results for both [Ru(terpy)(bpy)SCN]$^+$ isomerization and [Ru(terpy)(tbbpy)SCN]$^+$ isomerization, and the transition state scan for the [Ru(terpy)(tbbpy)SCN]$^+$ ion complex. This material is available free of charge via the Internet at http://pubs.acs.org.

■ AUTHOR INFORMATION

Corresponding Author

*E-mail: victor.batista@yale.edu (V.S.B.), robert.crabtree@yale.edu (R.H.C.).

■ ACKNOWLEDGMENTS

This material is based in part upon work supported as part of the Argonne-Northwestern Solar Energy Research (ANSER) Center, an Energy Frontier Research Center funded by the U.S. Department of Energy, Office of Science, Office of Basic Energy Sciences under Award Number DE-PS02-08ER15944 (T.P.B. synthesis, R.H.C., and V.S.B. PIs) and a catalysis grant from the Division of Chemical Sciences, Geosciences, and Biosciences, Office of Basic Energy Sciences of the U.S. Department of Energy through Grant DE-FG02-84ER13297 (N.D.S., crystallography). V.S.B also acknowledges supercomputing time

from NERSC. T.P.B. thanks Graham Dobereiner for many useful discussions.

REFERENCES

(1) Lewis, N. S. *Science* **2007**, *315*, 798.
(2) Grätzel, M. *Nature* **2001**, *414*, 338.
(3) O'Regan, B.; Grätzel, M. *Nature* **1991**, *353*, 737.
(4) Grätzel, M. *J. Photochem. Photobiol., C* **2003**, *4*, 145.
(5) Hagfeldt, A.; Boschloo, G.; Sun, L. C.; Kloo, L.; Pettersson, H. *Chem. Rev.* **2010**, *110*, 6595.
(6) Nazeeruddin, M. K.; De Angelis, F.; Fantacci, S.; Selloni, A.; Viscardi, G.; Liska, P.; Ito, S.; Bessho, T.; Grätzel, M. *J. Am. Chem. Soc.* **2005**, *127*, 16835.
(7) Nazeeruddin, M. K.; Pechy, P.; Renouard, T.; Zakeeruddin, S. M.; Humphry-Baker, R.; Comte, P.; Liska, P.; Cevey, L.; Costa, E.; Shklover, V.; Spiccia, L.; Deacon, G. B.; Bignozzi, C. A.; Grätzel, M. *J. Am. Chem. Soc.* **2001**, *123*, 1613.
(8) Nazeeruddin, M. K.; Kay, A.; Rodicio, I.; Humphry-Baker, R.; Muller, E.; Liska, P.; Vlachopoulos, N.; Grätzel, M. *J. Am. Chem. Soc.* **1993**, *115*, 6382.
(9) Ardo, S.; Meyer, G. J. *Chem. Soc. Rev.* **2009**, *38*, 115.
(10) Clifford, J. N.; Palomares, E.; Nazeeruddin, M. K.; Grätzel, M.; Durrant, J. R. *J. Phys. Chem. C* **2007**, *111*, 6561.
(11) Hamann, T. W.; Ondersma, J. W. *Energy Environ. Sci.* **2011**, *4*, 370.
(12) Tuikka, M.; Hirva, P.; Rissanen, K.; Korppi-Tommola, J.; Haukka, M. *Chem. Commun.* **2011**, *47*, 4499.
(13) Bhanuprakash, K.; Ghosh, S.; Chaitanya, G. K.; Nazeeruddin, M. K.; Grätzel, M.; Reddy, P. Y. *Inorg. Chem.* **2006**, *45*, 7600.
(14) Kohle, O.; Ruile, S.; Grätzel, M. *Inorg. Chem.* **1996**, *35*, 4779.
(15) Kohle, O.; Grätzel, M.; Meyer, A. F.; Meyer, T. B. *Adv. Mater.* **1997**, *9*, 904.
(16) Vandenburgh, L.; Buck, M. R.; Freedman, D. A. *Inorg. Chem.* **2008**, *47*, 9134.
(17) Homanen, P.; Haukka, M.; Luukkanen, S.; Ahlgren, M.; Pakkanen, T. A. *Eur. J. Inorg. Chem.* **1999**, 101.
(18) Homanen, P.; Haukka, M.; Pakkanen, T. A.; Pursiainen, J.; Laitinen, R. H. *Organometallics* **1996**, *15*, 4081.
(19) Tabatabaeian, K.; Adams, H.; Mann, B. E.; White, C. *J. Organomet. Chem.* **2003**, *688*, 75.
(20) Hadda, T. B.; Akkurt, M.; Baba, M. F.; Daoudi, M.; Bennani, B.; Kerbal, A.; Chohan, Z. H. *J. Enzym. Inhib. Med. Chem.* **2009**, *24*, 457.
(21) Hadda, T. B.; Le Bozec, H. *Inorg. Chim. Acta* **1993**, *204*, 103.
(22) Sullivan, B. P.; Calvert, J. M.; Meyer, T. J. *Inorg. Chem.* **1980**, *19*, 1404.
(23) Takeuchi, K. J.; Thompson, M. S.; Pipes, D. W.; Meyer, T. J. *Inorg. Chem.* **1984**, *23*, 1845.
(24) Maroney, M. J.; Fey, E. O.; Baldwin, D. A.; Stenkamp, R. E.; Jensen, L. H.; Rose, N. J. *Inorg. Chem.* **1986**, *25*, 1409.
(25) Herber, R. H.; Nan, G. J.; Potenza, J. A.; Schugar, H. J.; Bino, A. *Inorg. Chem.* **1989**, *28*, 938.
(26) Shklover, V.; Nazeeruddin, M. K.; Zakeeruddin, S. M.; Barbe, C.; Kay, A.; Haibach, T.; Steurer, W.; Hermann, R.; Nissen, H. U.; Grätzel, M. *Chem. Mater.* **1997**, *9*, 430.
(27) Frisch, M. J.; Trucks, G. W.; Schlegel, H. B.; Scuseria, G. E.; Robb, M. A.; Cheeseman, J. R.; Scalmani, G.; Barone, V.; Mennucci, B.; Petersson, G. A.; Nakatsuji, H.; Caricato, M.; Li, X.; Hratchian, H. P.; Izmaylov, A. F.; Bloino, J.; Zheng, G.; Sonnenberg, J. L.; Hada, M.; Ehara, M.; Toyota, K.; Fukuda, R.; Hasegawa, J.; Ishida, M.; Nakajima, T.; Honda, Y.; Kitao, O.; Nakai, H.; Vreven, T.; Montgomery, J., J. A.; Peralta, J. E.; Ogliaro, F.; Bearpark, M.; Heyd, J. J.; Brothers, E.; Kudin, K. N.; Staroverov, V. N.; Kobayashi, R.; Normand, J.; Raghavachari, K.; Rendell, A.; Burant, J. C.; Iyengar, S. S.; Tomasi, J.; Cossi, M.; Rega, N.; Millam, N. J.; Klene, M.; Knox, J. E.; Cross, J. B.; Bakken, V.; Adamo, C.; Jaramillo, J.; Gomperts, R. E.; Stratmann, O.; Yazyev, A. J.; Austin, R.; Cammi, C.; Pomelli, J. W.; Ochterski, R.; Martin, R. L.; Morokuma, K.; Zakrzewski, V. G.; Voth, G. A.; Salvador, P.; Dannenberg, J. J.; Dapprich, S.; Daniels, A. D.; Farkas, O.; Foresman, J. B.; Ortiz, J. V.; Cioslowski, J.; Fox, D. J. *Gaussian 09*, revision A.02; Gaussian Inc.: Wallingford, CT, 2004.
(28) Tomasi, J.; Mennucci, B.; Cammi, R. *Chem. Rev.* **2005**, *105*, 2999.
(29) Marenich, A. V.; Cramer, C. J.; Truhlar, D. G. *J. Phys. Chem. B* **2009**, *113*, 6378.